Catalytic behavior of vanadium-containing mesoporous silicas in the oxidative dehydrogenation of propane

José Santamaría-González, Joaquín Luque-Zambrana, Josefa Mérida-Robles, Pedro Maireles-Torres, Enrique Rodríguez-Castellón and Antonio Jiménez-López *

Departamento de Química Inorgánica, Cristalografía y Mineralogía, Facultad de Ciencias, Universidad de Málaga, Campus de Teatinos, 29071 Málaga, Spain

Received 1 February 2000; accepted 27 May 2000

Three series of vanadium-containing silica catalysts (2–7.6 wt% V) have been prepared by varying the synthesis method. In all cases, conversion values in the oxidative dehydrogenation of propane increase with the temperature, vanadium loading and reducibility. For impregnated and anchored catalysts, a relationship between the selectivity towards propene and the effective acidity, as determined in the dehydration of 2-propanol, can be established.

Keywords: vanadium-based catalysts, mesoporous vanadosilicates, oxidative dehydrogenation of propane, MCM-41

1. Introduction

The increasing need of upgrading low-cost feedstocks has greatly prompted the research on the selective oxidation reactions of light alkanes, as an alternative to the use of the more expensive olefins. In this sense, much attention has been recently paid to the oxidative dehydrogenation (ODH) of alkanes, mainly from C_2 to C_4, to give the corresponding alkenes [1–3], which can be carried out at an easier thermal control than in the pure dehydrogenation, thus minimizing the undesired collateral reactions.

Supported vanadium oxides have been extensively studied as selective catalysts in ODH reactions [4–8]. It has been established that parameters such as the oxidation state, coordination number, aggregation state and reducibility of vanadium species, distance between active sites or the acid/base properties of the catalysts have to be taken into account in order to explain the observed catalytic behavior. Furthermore, this also seems to be influenced by the vanadium loading since the degree of aggregation of the VO_4 units depends on this. The best catalytic performance and selectivity for the ODH reaction of alkanes has been attributed to the presence of isolated tetrahedral V(V) species, whereas polymeric vanadium species could favor undesired reactions, leading to the formation of carbon oxides.

Recently, the discovery of a new family of molecular sieves [9], generically denominated as M41S, has opened new and exciting possibilities in the catalysis and sorption fields [10,11]. These mesoporous materials usually exhibit a great versatility in terms of both chemical nature and structural characteristics. Thus, the synthesis, characterization and catalytic properties of V-doped mesoporous silica have been extensively reported [12–17].

The present work is aimed to study the influence of the vanadium incorporation method in a mesoporous silica framework, on the catalytic performance of vanadium-containing mesoporous silica catalysts in the oxidative dehydrogenation of propane. Three synthetic strategies have been used: (i) impregnation of silica MCM-41, (ii) anchoring of vanadium species on silica MCM-41, and (iii) structurally doping in the synthesis step. The catalytic results will be rationalized in terms of acid properties of the catalysts as well as the nature, dispersion degree and reducibility of vanadium species.

2. Experimental

2.1. Synthesis of catalysts

The synthesis of vanadium-impregnated mesoporous silica has been performed by treating a mesoporous silica MCM-41 support, synthesized according to the literature [9], with a $VOSO_4$ aqueous solution by using the incipient wetness method (1 g of calcined Si-MCM-41 support and different amounts of $VOSO_4 \cdot 5H_2O$ dissolved in 2 cm^3 of H_2O, in order to attain loading of 2, 3, 4.5 and 6 wt% of V). After solvent evaporation, the V-impregnated silica catalysts were obtained by calcination in air at 823 K, and they will be hereinafter called V-2i, V-3i, V-4.5i and V-6i catalysts.

A second method of vanadium incorporation has been carried out by anchoring vanadium(V) species on a MCM-41 silica previously dehydrated at 393 K in air for 24 h. This support was soaked with $VOCl_3$ dissolved in *n*-hexane under a nitrogen stream. Thus, catalysts with 2–6 wt% of V have been synthesized (1 g of calcined Si-MCM-41 support and different amounts $VOCl_3$ dissolved in 0.98 cm^3

* To whom correspondence should be addressed.

of n-hexane), rinsed with n-hexane in order to remove the possible excess of $VOCl_3$ and finally treated at 823 K to obtain the catalysts labeled as V-2a, V-3a, V-4.5a and V-6a, respectively.

Finally, mesoporous vanadium-doped MCM-41 materials were synthesized as follows: different volumes of a vanadyl(IV) sulfate aqueous solution were added to a mixture of cetyltrimethylammonium chloride (CTMACl) and Na_2SiO_3/Cab-O-Sil in order to attain Si/V atomic ratios of 10 and 25. The pH was then adjusted to 11 by adding a tetramethylammonium hydroxide (TMAOH) aqueous solution. The resulting gel of molar composition $1.00SiO_2 : xV_2O_5 : 0.48CTMACl : 0.96Na_2O : 3.70TMAOH : 222H_2O$, with $x = 0.02$ (V25) or 0.05 (V10), was firstly stirred at room temperature for 1 day, and then under hydrothermal conditions for 3 days. Finally, the solid was recovered by centrifugation, washed with water and ethanol and air-dried at 333 K. V10 and V25 catalysts were obtained after removing the surfactant species by calcining the precursor solids at 823 K.

2.2. Characterization methods

Chemical analyses of V were done by colorimetry ($\lambda =$ 460 nm) by the formation of the orange $H_3V_2O_7^-$ in acid medium with $KMnO_4$ as oxidant. Catalysts were previously treated with a HF aqueous solution [18].

X-ray diffraction patterns were collected with a Siemens D501 diffractometer (Cu K_α source) provided with a graphite monochromator. UV-vis spectroscopy studies were carried out in the diffuse reflectance mode with a Shimadzu MPC 3100 spectrophotometer and $BaSO_4$ as reference. The X-ray photoelectron spectra (XPS) were recorded with a Physical Electronics 5700 instrument, the band-pass energy being 29.35 eV. The Mg K_α X-ray excitation source ($h\nu = 1253.6$ eV) was at a power of 300 W. The pressure in the analysis chamber was maintained below 1.3×10^{-7} Pa during data acquisition. The binding energies (BE) were obtained with ± 0.2 eV accuracy and charge compensation done with the adventitious C 1s peak at 248.8 eV.

N_2 adsorption–desorption isotherms were determined in a glass conventional volumetric apparatus at 77 K, outgassing previously the samples at 473 K and 10^{-2} Pa overnight. Pore size distributions were calculated by using the Cranston and Inkley method for cylindrical pores [19].

Temperature-programmed desorption of ammonia (NH_3-TPD) was used to determine the total acidity of the samples. The nature of acid sites was determined by pyridine adsorption coupled to infrared spectroscopy. Both methods have been described in detail elsewhere [20]. The effective acidity of the catalysts [21] has been studied by using the conversion of 2-propanol as probe reaction, performing catalytic runs at 493 K in a fixed-bed quartz U-tube microreactor working at atmospheric pressure, containing ca. 0.03 g of catalyst without dilution.

Hydrogen temperature-programmed reduction (H_2-TPR) of the catalysts was carried out between 393 and 973 K, using a flow of Ar/H_2 (40 $cm^3\,min^{-1}$, 10% of H_2) and a heating rate of 10 K/min. Water produced in the reduction reaction was eliminated by passing the gas flow through a cold finger (193 K). The consumption of hydrogen was controlled by an on-line gas chromatograph provided with a TCD.

The catalysts were tested in the oxidative dehydrogenation of propane, using an automatic microcatalytic flow reactor working at atmospheric pressure. A fixed-bed quartz U-tube reactor with a catalyst charge ranging from 0.015 to 0.120 g without dilution was used. Samples were previously treated at 773 K, under a He flow (30 $cm^3\,min^{-1}$) for 1 h. The gas reaction mixture was constituted of 7.06 mol% propane in O_2/N_2 (19.51/73.41 mol%) and a total flow rate equal to 28.32 $cm^3\,min^{-1}$. The contact times (W/F) were varied between 3.1 and 24.5 $g_{cat}\,h\,mol\text{-}propane^{-1}$. Under these conditions, both external and internal diffusional limitations were absent. Analysis of the products was performed using on-line gas chromatography with a Shimadzu GC-14B provided with a column (7 m in length and $1/8''$ internal diameter) filled with sebaconitrile and using a flame ionization detector. The analysis of CO_2 was carried out on line with a packed column Porapack Q (2.5 m in length, $1/8''$ OD) and a TCD.

3. Results and discussion

3.1. Characterization of catalysts

The vanadium contents of the vanadium-based catalysts (table 1) reveal that almost all vanadium is incorporated into the inorganic framework, except for the anchored catalysts with high vanadium content where the vanadium added probably exceeds the number of available anchoring sites. The powder X-ray diffraction patterns show, in all cases, the characteristic low-angle diffraction peak (ca. 37 Å), which is attributed to the d_{100} reflection assuming a hexagonal lattice, typical of MCM-41 solids. The absence of diffraction peaks at 2θ angles higher than 10° seems to discard the presence of V_2O_5 crystallites, thus pointing to a homogeneous distribution of the vanadium species.

Diffuse reflectance electronic spectroscopy allows us to shed light into the oxidation state and geometry of vanadium species. By comparing the spectra of $VOSO_4$, V_2O_5 and as-synthesized and calcined V10 materials (figure 1), it can be inferred that V_2O_5 is absent in this catalyst, because the band at 510 nm, characteristic of octahedral vanadium(V) in the V_2O_5 crystallites, is not observed [22]. Moreover, the diffuse reflectance spectrum of the as-synthesized V10 sample exhibits a weak absorption at 610 nm which can be attributed to V(IV) ions, as confirmed by the green color of the as-synthesized V10 material, which is indicative of the presence of VO^{2+} ions, although in minor amounts. After calcination at 823 K (catalyst V10), this band completely disappears and the DR curve only exhibits two features associated to charge transfer bands at 270 and 340 nm, assigned to V–O transfer

Table 1
Main characteristics of the vanadium-containing silica catalysts.

Catalyst	V (wt%)	d_{100} (Å)	S_{BET} ($m^2\,g^{-1}$)	V_p ($cm^3\,g^{-1}$)	Reduction temperature (K)	Total acidity (mmol-$NH_3\,g^{-1}$)	Catalytic activity (2-propanol conversion) (μmol-$C_3H_6\,g^{-1}\,s^{-1}$)
Si-MCM41	–	37.0	806	0.603	–	0.52	0
V-2i	1.8	37.2	804	0.509	792	0.72	0.77
V-3i	3.1	36.4	719	0.539	771	0.81	1.08
V-4.5i	4.4	36.0	647	0.713	742	1.00	2.63
V-6i	6.1	36.6	518	0.681	742	1.17	3.84
V-2a	1.9	38.6	714	0.543	788	0.93	0.70
V-3a	2.8	36.6	751	0.473	781	1.47	0.85
V-4.5a	4.2	–	652	0.509	727	1.52	1.89
V-6a	5.0	–	637	0.530	722	1.59	2.47
V10	7.6	36.7	714	0.584	822	1.78	1.87
V25	2.5	38.1	727	0.740	791, 821, 862	1.30	0.53

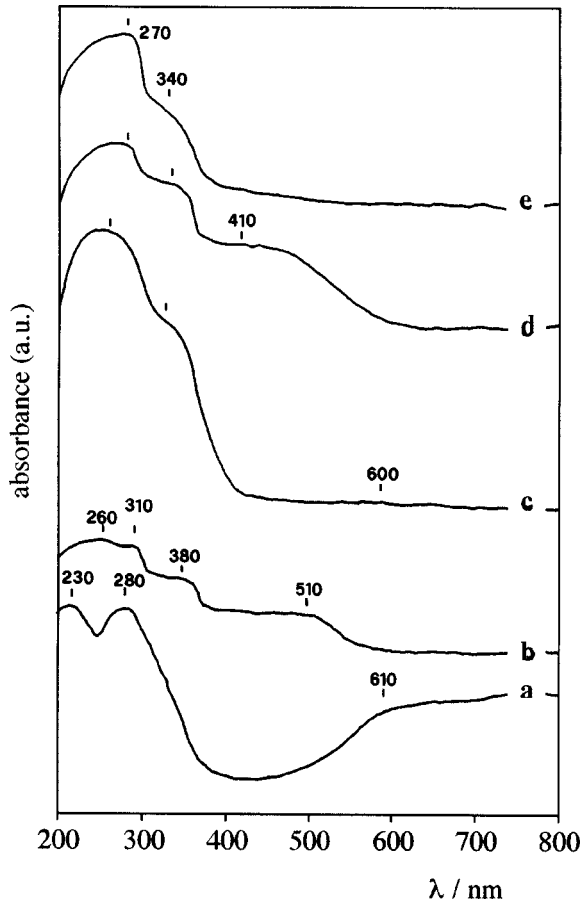

Figure 1. Diffuse reflectance UV-vis spectra of (a) $VOSO_4$, (b) V_2O_5, (c) as-synthesized V10, (d) hydrated V10 and (e) dehydrated V10 catalysts.

$\pi t_2 \rightarrow e$ and $\pi t_1 \rightarrow e$, respectively, in tetrahedral V(V) species [13]. If the V10 catalyst is exposed to humidity, a new band at 410 nm appears, which can be attributed to the absorption of water and the formation of square pyramidal V(V), a process which is accompanied by a color change from white to yellow [13,15]. This coordination of water molecules is completely reversible. The diffuse reflectance spectra of impregnated and anchored vanadium catalysts are quite similar to that of structurally vanadium-doped catalysts.

The XPS curves in the V 2p region of the as-synthesized vanadium-containing solids show, after O 1s satellite subtraction, an asymmetric peak which can be deconvoluted in two components. The maxima at 515.5 and 517.1 eV reveal the coexistence of vanadium species in oxidation state IV and V, respectively. After calcination, the peak at 515.5 eV remains, which could be due to a partial reduction of V(V) when exposing the samples to the X-ray beam.

Nitrogen adsorption–desorption isotherms at 77 K are almost reversible type IV in the IUPAC classification, typical feature of MCM-41 mesoporous solids. S_{BET} values are high and ranged between 518 and 727 $m^2\,g^{-1}$, being, in general, lower than that found for the siliceous support (806 $m^2\,g^{-1}$) (table 1). The vanadium-anchored catalysts exhibit isotherms with some hysteresis loops, the existence of which could be related to the process of vanadium incorporation, where evolved HCl can damage the structure. Pore size distribution curves of the different catalysts show a single peak corresponding to average pore radii ranging between 11.2 and 16.2 Å.

Hydrogen temperature-programmed reduction patterns of the catalysts (table 1) indicate that impregnated and anchored catalysts with the similar vanadium loading have almost the same reduction temperature, assigned to the reduction process of V(V) to V(III) [23]. But, in both series of catalysts, the temperature of the maximum of hydrogen consumption decreases with the vanadium content (figure 2). This behavior has been also observed by Blasco et al. in the VO_x/Al_2O_3 system [24]. Regarding the structurally vanadium-doped catalysts, they seem to be more resistant to the reduction process since it takes place at higher temperature and in a more large interval of temperatures, which might reflect the existence of vanadium in different environments. However, the formation of V_2O_5 crystallites, which can be monitored by a sharp peak at ca. 923 K, has never been detected.

On the other hand, the comparison of the temperature-programmed desorption curves of ammonia of the support and the V10 catalyst (figure 3) allows us to indicate that incorporation of vanadium provokes a moderate development of acidity. Indeed, ammonia molecules are only re-

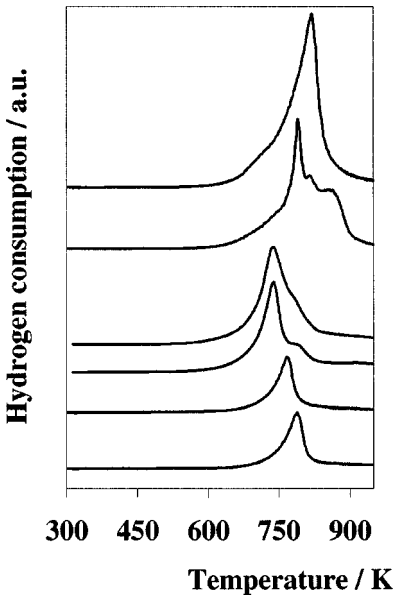

Figure 2. TPR profiles of the hydrogen consumption (from top to bottom) of V10, V25, V-6a, V-4.5a, V-3a and V-2a catalysts.

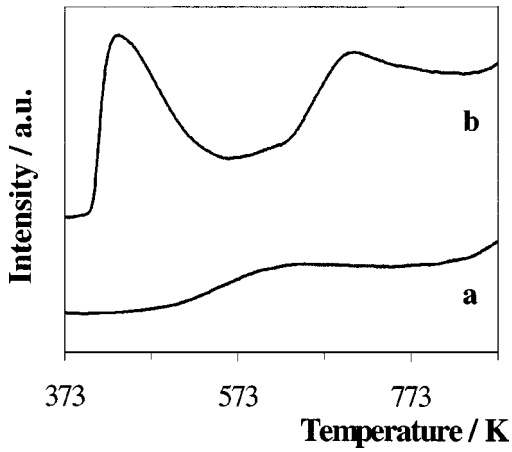

Figure 3. Curves of temperature-programmed desorption of ammonia corresponding to (a) Si-MCM-41 and (b) V10 materials.

moved from siliceous support at temperatures higher than 473 K, the total amount of desorbed ammonia until 873 K being 0.52 mmol g^{-1}. These acid sites could be assigned to silanol groups, of which the O–H strength vibration is observed in its infrared spectrum (figure 4) at 3751 cm^{-1}. However, the total acidity found for the V10 catalyst attains a value of 1.78 mmol-NH_3 g^{-1}. The incorporation of vanadium species by structural doping leads to the appearance of a new band in the NH_3-TPD curve at ca. 433 K, which can be due to the enhancement of acid strength of silanol groups provoked by the presence of surrounding vanadium species. Moreover, the infrared spectrum of the V10 catalyst (figure 4) shows a new band at 3664 cm^{-1} which probably corresponds to OH strength vibration of VOH groups. The lower energy of this band indicates that these acid groups are stronger than Si–OH groups, and they would be responsible of the ammonia desorption band centered at ca. 700 K.

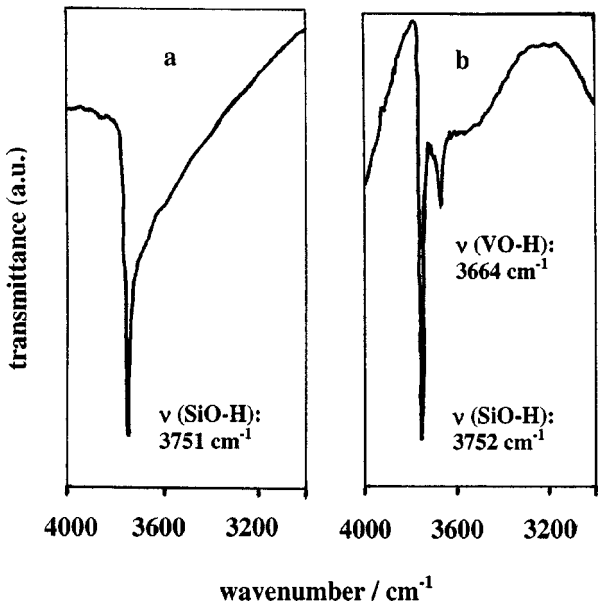

Figure 4. Infrared spectra in the region 3000–4000 cm^{-1} of (a) Si-MCM-41 and (b) V10 catalysts.

For the other catalysts, the total acidity ranges between 0.72 and 1.59 mmol g^{-1}, the vanadium-anchored samples being more acidic than those impregnated (table 1).

By pyridine adsorption coupled to IR spectroscopy has been established that the majority of acid sites are of Brønsted type (absorption band at 1550 cm^{-1}). However, after outgassing at 493 K, the catalysts do not contain adsorbed pyridine. The absence of Lewis acid sites contrasts with the observed capacity of the superficial vanadium species to absorb water to increase their coordination number. Therefore, it could be possible that pyridine molecules are preferentially adsorbed on Brønsted V–OH acid sites and so impede their direct coordination to vanadium atoms.

The acid characterization of these vanadium-containing samples has been completed by evaluating their performance in the catalytic reaction of 2-propanol conversion at 493 K. This reaction has been chosen as a test reaction in order to evaluate the effective acidity of the active sites. It is well established that acid sites produce propene (dehydration reaction), whereas basic and redox sites are responsible for the production of acetone (dehydrogenation reaction). The activity values (table 1) are low and range between 0.53 and 3.84 μmol-propene g^{-1} s^{-1}, and, in all cases, the unique reaction product was propene with a selectivity close to 100%. Taking into account that the pristine silica MCM-41 is completely inactive in this reaction, the incorporation of vanadium species is responsible of their observed catalytic activities.

3.2. Catalytic activity

The catalytic behavior in the ODH reaction of propane for the three series of vanadium-containing catalysts: impregnated, anchored and structurally doped, has been eval-

uated between 723 and 823 K. Silica MCM-41 support is also inactive in this reaction under all the experimental conditions. The only products detected were always propene, CO and CO_2; nevertheless ethane, ethene and methane were found as traces at high reaction temperature and high conversion levels of propane.

In the case of vanadium-impregnated catalysts, from the variation of propane conversion with the reaction temperature (figure 5), it can be deduced that propane conversion increases with both the temperature, especially above 773 K, and with the vanadium loading. Moreover, the easy reduction of vanadium species, as inferred from H_2-TPR data (table 1), might be considered to explain the trend of the catalytic results. However, although conversions increase with the temperature, the yields of propene change in a different way along this group of catalysts, being very similar for samples with vanadium loading higher than 3 wt% (table 2). This is a consequence of a different evolution of propene selectivity with temperature, which strongly decreases at high conversions for samples with maximum vanadium loadings (figure 6). Only the sample with 2 wt% of vanadium exhibits an always increasing selectivity with temperature. Turnover frequency numbers, considering the activity per atom of vanadium, also decrease with vanadium loadings (table 2).

The selectivities to CO and CO_2 for vanadium-impregnated catalysts are very high for CO with values comprised between 60 and 75%, while for CO_2 they increase with the conversion, but they always are lower than 25% (table 2). This should be explained by considering that CO is both a primary and secondary product, while CO_2 is essentially a secondary product in the oxidative reaction of propene. Furthermore, the evolution of the selectivity to CO_2 with the vanadium loading matches very well with the total acidity. Thus, while the total acidity increases from 0.72 to 1.17 mmol g^{-1}, the selectivity to CO_2 goes from 2.3 to 20.3%. Therefore, the higher the acidity the higher is the total oxidation, which can be justified by the strong retention of the olefin intermediate on these acid sites and its ulterior oxidation to CO_2 [25–27].

It is well known that selectivity of alkane dehydrogenation in oxidative conditions is a function of the type of vanadium species present on the catalyst. Thus, it has been established that isolated or polymeric tetrahedral V(V) species are the most selective to alkene formation [2,28]. On the other hand, the nature of the vanadium species deposited onto the surface of a given support depends upon the vanadium loading and the acid–base properties of such support. In fact, the formation of V_2O_5 crystallites on the silica surface has been already detected at a coverage degree only higher than 10% of the theoretical monolayer. The weak

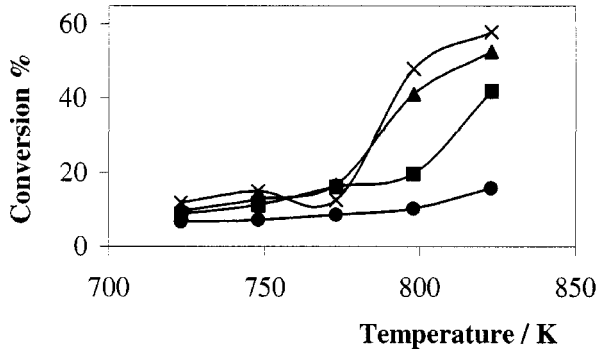

Figure 5. Variation of the propane conversion as a function of the reaction temperature during the ODH of propane on vanadium-impregnated silica MCM catalysts: V-2i (●), V-3i (■), V-4.5i (▲) and V-6i (×). $W/F = 24.5$ g h mol-C_3^{-1}.

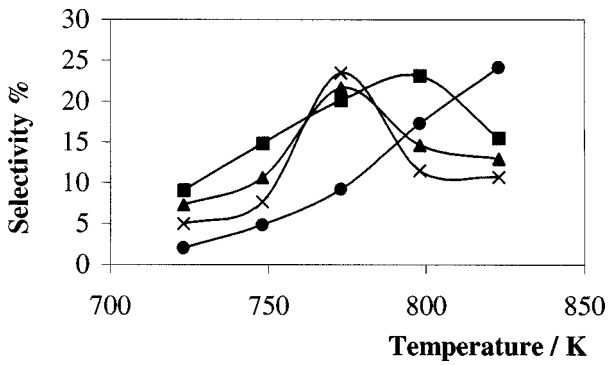

Figure 6. Dependence of selectivity to propene on the reaction temperature in the ODH of propane for vanadium-impregnated silica MCM catalysts: V-2i (●), V-3i (■), V-4.5i (▲) and V-6i (×). $W/F = 24.5$ g h mol-C_3^{-1}.

Table 2
Catalytic results for ODH of propane over vanadium-based catalysts at 823 K.[a]

Catalyst	Conversion (%)	TOF × 10^{21} (μmol-C_3H_6 s^{-1} at-V^{-1})	Selectivity (%)			Propene yield (%)
			Propene	CO	CO_2	
V-2i	15.8	6.79	24.1	73.3	2.3	3.8
V-3i	42.0	6.74	15.5	71.0	12.4	6.5
V-4.5i	52.6	4.98	13.0	66.7	20.3	6.8
V-6i	57.9	3.27	10.8	70.1	19.1	6.2
V-2a	25.3	8.71	20.4	73.4	5.7	5.2
V-3a	28.1	5.52	17.2	73.1	9.3	4.8
V-4.5a	49.1	6.53	17.2	61.5	20.6	8.6
V-6a	56.5	4.79	13.2	61.0	24.5	7.5
V10	28.8	2.37	19.5	72.1	8.1	5.6
V25	40.3	8.12	15.7	67.4	15.3	6.3

[a] $W/F = 24.5$ g h mol-C_3^{-1}.

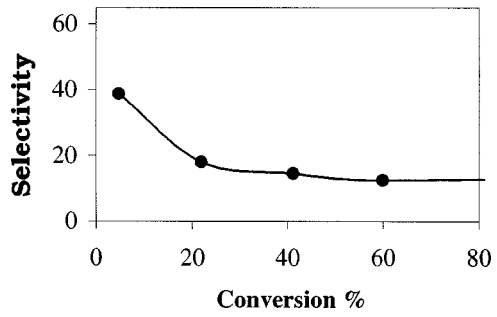

Figure 7. Propene selectivity as a function of the propane conversion on V-4.5i catalyst at 798 K.

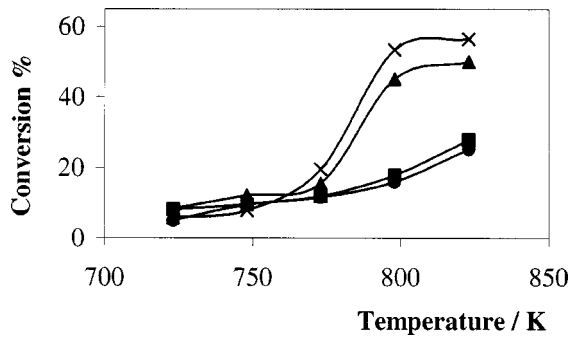

Figure 8. Variation of the conversion of propane versus reaction temperature for vanadium-anchored silica MCM catalysts: V-2a (•), V-3a (■), V-4.5a (▲) and V-6a (×). $W/F = 24.5$ g h mol-C_3^{-1}.

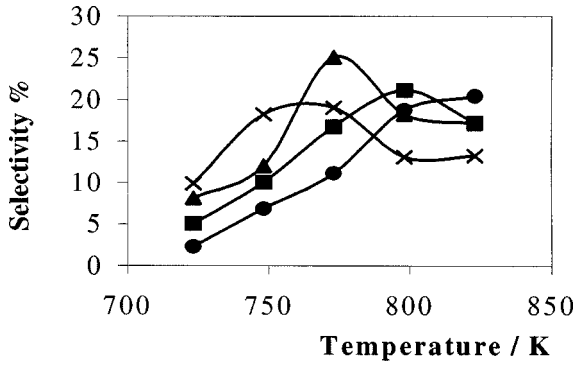

Figure 9. Dependence of selectivity to propene on the reaction temperature in the ODH of propane for vanadium-anchored silica MCM catalysts: V-2a (•), V-3a (■), V-4.5a (▲) and V-6a (×). $W/F = 24.5$ g h mol-C_3^{-1}.

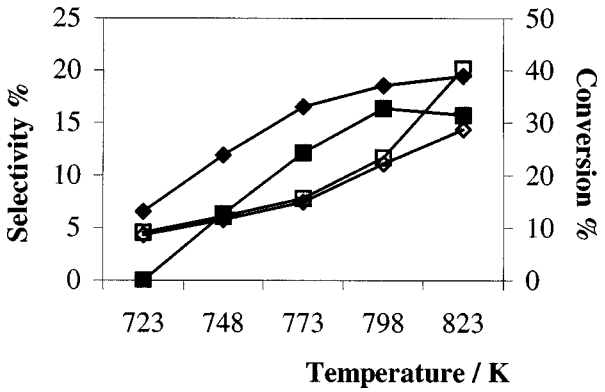

Figure 10. Variation of the conversion of propane (open symbols) and the selectivity to propene (closed symbols) versus the reaction temperature for structurally vanadium-doped silica MCM catalysts: V10 (♦, ◊) and V25 (■, □). $W/F = 24.5$ g h mol-C_3^{-1}.

interaction between vanadium species and the support is the origin of this lower dispersion degree [29]. For our impregnated vanadium silica MCM catalysts, due to the high surface area of the support, the coverage degrees attained were very low, between 0.035 and 0.08 of a monolayer, considering 4.98×10^{18} molecules of V_2O_5 per square meter as the amount necessary to form a monolayer on a support. These data theoretically might lead to a good dispersion of vanadium species, which in turn is supported by the characterization results, where only tetrahedral V(V) species were detected. Concerning the selectivities to propene, they decrease with conversion, as can be observed for the sample with 4.5 wt% V (figure 7). This means that the formation of the secondary product, CO_2, largely increases at the expense of propene with conversion. In this way, the experimental data seem to indicate the formation of a large number of V(IV) species at high conversion levels which can be responsible of the low propene selectivity values, as has been observed in the ODH of alkanes over supported vanadium catalysts [24]. This assumption is quite probable taking into account the reducing atmosphere around the active centers owing to the high percentage of CO formed during the ODH of propane.

For vanadium-anchored catalysts, the variation of the conversion and the selectivity to propene as a function of the temperature (figures 8 and 9) exhibits a similar behavior to that observed for impregnated samples. This fact is expected by considering the strong analogies found in the characterization between both groups of catalysts. However, the selectivity values and the propene yields are generally higher for anchored vanadium materials (table 2). These differences could appear as a consequence of the acidic properties of both groups of catalysts. Thus, although the total acidity of anchored vanadium catalysts, as determined from NH_3-TPD, is higher than those of impregnated analogs, the effective acidity as probed in the dehydration reaction of 2-propanol is lower. The higher effective acidity of vanadium-impregnated catalysts is well correlated with the lower selectivity to propene in the ODH of propane. This relationship has been already observed in ODH of ethane on chromium-containing oxides pillared zirconium phosphate materials [20]. In fact, the higher the effective acidity, the higher the retention of propene molecules, which leads to their total oxidation to carbon oxides, thus giving rise to a lower selectivity to propene.

Concerning the catalytic behavior of the two structurally vanadium-doped silica MCM-41 catalysts, with vanadium contents of 2.5 and 7.6 wt%, the catalytic results indicate that an increase in the vanadium content does not result in a better performance in the ODH of propane (figure 10 and table 2). Furthermore, differences in conversion and selectivity are found in comparison with anchored or impregnated catalysts with similar vanadium content. This

behavior is expected taking into account the structural, textural and acid characteristics of these catalysts, which differ from those of impregnated and anchored catalysts. This difference could be explained by both, a more difficult reducibility of these catalysts, because the peaks of hydrogen consumption appear at higher temperature, and the existence of a fraction of vanadium atoms which are located into the walls of the silica MCM-41 framework in sites of difficult access to the propane molecules.

4. Conclusions

Impregnation or anchoring of vanadium species gives rise to catalysts which exhibit similar textural and reduction features, whereas the structural doping in the synthesis step gives rise to more crystalline mesoporous solids where vanadium centers are reduced at higher temperature. The catalytic performances in the ODH reaction of propane seem to be relatively independent of the incorporation method of the active phase in the case of anchored and impregnated samples, but different when vanadium is structurally incorporated in the synthesis step. A plausible relationship between the selectivity to propene and the effective acidity of catalysts can be proposed.

Acknowledgement

We thank the CICYT (Spain), project MAT97-906, for financial support.

References

[1] H.H. Kung, Adv. Catal. 40 (1994) 1.
[2] M.M. Bettahar, G. Costentin, L. Savary and J.C. Lavalley, Appl. Catal. A 145 (1996) 1.
[3] T. Blasco and J.M. López-Nieto, Appl. Catal. A 157 (1997) 117.
[4] A. Parmaliana, V. Sokolovskii, D. Miceli and N. Giordano, Appl. Catal. A 135 (1996) L1.
[5] A. Corma, J.M. López-Nieto and N. Paredes, J. Catal. 144 (1993) 425.
[6] X. Gao, P. Ruiz, Q. Xim, X. Guo and B. Delmon, J. Catal. 148 (1994) 56.
[7] U. Schart, M. Scharmi-Marth, A. Wokaun and A. Baiker, J. Chem. Soc. Faraday Trans. 87 (1991) 4299.
[8] M. Sato, M. Toita, T. Sodesawa and F. Nozaki, Appl. Catal. 62 (1990) 73.
[9] J.S. Beck, J.C. Vartuli, W.J. Roth, M.E. Leonowicz, C.T. Kresge, K.D. Schmitt, C.T.W. Chu, D.H. Olsen, E.W. Sheppard, S.B. McCullen, J.B. Higgins and J.L. Schlenker, J. Am. Chem. Soc. 114 (1992) 10834.
[10] A. Sayari, Chem. Mater. 8 (1996) 1840.
[11] A. Corma, Chem. Rev. 97 (1997) 2373.
[12] J.S. Reddy, P. Liu and A. Sayari, Appl. Catal. A 148 (1996) 7.
[13] K.J. Chao, C.N. Wu, H. Chang, L.J. Lee and S.F. Hu, J. Phys. Chem. B 101 (1997) 6341.
[14] M. Chatterjee, T. Iwasaki, H. Hayashi, Y. Onodera, T. Ebina and T. Nagase, Chem. Mater. 11 (1999) 1368.
[15] Z. Luan, J. Xu, H. He, J. Klinowski and L. Kevan, J. Phys. Chem. B 100 (1996) 19595.
[16] G. Grubert, J. Rathouský, G. Schulz-Ekloff, M. Wark and A. Zukal, Micropor. Mesopor. Mater. 22 (1998) 225.
[17] D.H. Park, C.F. Cheng, H.Y. He and J. Klinowski, J. Mater. Chem. 7 (1997) 159.
[18] G. Charlot, *Chimie Analytique Quantitative*, Vol. II, *Méthodes Sélectionnées d'Analyse Chimique des Éléments* (Masson, Paris, 1974).
[19] R.W. Cranston and F.A. Inkley, Adv. Catal. 9 (1957) 143.
[20] B. Solsona, J.M. López-Nieto, M. Alcántara-Rodríguez, E. Rodríguez-Castellón and A. Jiménez-López, J. Mol. Catal. 153 (2000) 199.
[21] R. Grabowski, B. Grybowska, K. Samson, J. Slolzinski, J. Stoch and Wcislo, Appl. Catal. A 125 (1995) 129.
[22] A.B.P. Lever, *Inorganic Electronic Spectroscopy*, 2nd Ed. (Elsevier, Amsterdam, 1984).
[23] F. Arena, F. Frusteri and A. Parmaliana, Appl. Catal. A 176 (1999) 189.
[24] T. Blasco, A. Galli, J.M. López-Nieto and F. Trifirò, J. Catal. 169 (1997) 203.
[25] A. Galli, J.M. López-Nieto, A. Dejoz and M.I. Vázquez, Catal. Lett. 34 (1995) 51.
[26] P. Concepción, A. Galli, J.M. López-Nieto, A. Dejoz and M.I. Vázquez, Topics Catal. 3 (1996) 451.
[27] T. Blasco, A. Dejoz, J.M. López-Nieto and M.I. Vázquez, J. Catal. 157 (1997) 271.
[28] E.A. Mamedov and V. Cortés-Corberán, Appl. Catal. A 127 (1995) 1.
[29] J.M. López-Nieto, G. Kremenic and J.L.G. Fierro, Appl. Catal. 61 (1990) 235.